⌘ *Author's Choice*

THE JOURNAL OF BIOLOGICAL CHEMISTRY VOL. 287, NO. 53, pp. 44270–44277, December 28, 2012

Laminin Network Formation Studied by Reconstitution of Ternary Nodes in Solution*

Received for publication, September 10, 2012, and in revised form, October 22, 2012 Published, JBC Papers in Press, November 19, 2012, DOI 10.1074/jbc.M112.418426

Alan Purvis and Erhard Hohenester[1]

From the Department of Life Sciences, Imperial College London, London SW7 2AZ, United Kingdom

Background: Laminin self-assembly into a cell-associated network is essential for basement membrane formation.
Results: The isolated tips of the laminin short arms form ternary complexes in solution.
Conclusion: The nodes in the laminin network are formed by the N-terminal domains of one α, one β, and one γ chain.
Significance: The reconstitution of laminin network nodes enables structure-function studies.

The polymerization of laminins into a cell-associated network is a key process in basement membrane assembly. Network formation is mediated by the homologous short arm tips of the laminin heterotrimer, each consisting of a globular laminin N-terminal (LN) domain followed by a tandem of laminin-type epidermal growth factor-like (LEa) domains. How the short arms interact in the laminin network is unclear. Here, we have addressed this question by reconstituting laminin network nodes in solution and analyzing them by size exclusion chromatography and light scattering. Recombinant LN-LEa1–4 fragments of the laminin α1, α2, α5, β1, and γ1 chains were monomeric in solution. The β1 and γ1 fragments formed the only detectable binary complex and ternary complexes of 1:1:1 stoichiometry with all α chain fragments. Ternary complex formation required calcium and did not occur at 4 °C, like the polymerization of full-length laminins. Experiments with chimeric short arm fragments demonstrated that the LEa2–4 regions of the β1 and γ1 fragments are dispensable for ternary complex formation, and an engineered glycan in the β1 LEa1 domain was also tolerated. In contrast, mutation of Ser-68 in the β1 LN domain (corresponding to a Pierson syndrome mutation in the closely related β2 chain) abolished ternary complex formation. We conclude that authentic ternary nodes of the laminin network can be reconstituted for structure-function studies.

Basement membranes are extracellular matrices that underlie all epithelial cell sheets and surround muscle, peripheral nerve, and fat cells (1). An invariant constituent of basement membranes is laminin, which self-assembles into a cell-associated network. A second network is subsequently formed by type IV collagen and is connected to the laminin network by nidogen, perlecan, and agrin (1). The self-assembly of laminin is a critical step in basement membrane formation, without which cell differentiation and tissue formation cannot proceed (2).

The 16 mammalian laminins are heterotrimers that are assembled from one of five α chains, one of three β chains, and one of three γ chains (3). Laminins are cross-shaped molecules (4). The long arm of the cross is a coiled coil of all three chains that terminates in a cell-adhesive globular region contributed by the α chain. The three short arms consist of one chain each and are composed of a laminin N-terminal (LN)[2] domain followed by tandem repeats of laminin-type epidermal growth factor-like (LE) domains, interspersed with one or two globular domains of unknown structure. The process of laminin polymerization has been extensively studied using laminin-111 (α1β1γ1) isolated from the mouse Engelbreth-Swarm-Holm tumor and, more recently, recombinant laminin heterotrimers (5–12). Laminin polymerization in solution occurs by a nucleation-propagation mechanism and requires calcium; like tubulin, laminin can be depolymerized by cooling to 4 °C. According to the "three-arm interaction model" (10), the nodes in the laminin network are assembled cooperatively from the short arm tips of one α, one β, and one γ chain (see Fig. 1*A*). However, this model was called into question by one study that reported strong and promiscuous pairwise interactions between laminin short arms (13).

We recently determined crystal structures of the short arm tips of the laminin α5, β1, and γ1 chains (14, 15). The LN domain is a β-sandwich with several long loops that is attached like the head of a sunflower to a stalk made up of the disulfide-rich LE domains. One face of the LN domain is highly conserved in each of the three chain subfamilies, suggesting that these might be the surfaces involved in network formation. Indeed, mutation of several conserved residues in the α5 LN domain abrogated the ability of the recombinant fragment to inhibit laminin polymerization (15). When we examined the interactions between the crystallized laminin short arm fragments using surface plasmon resonance (SPR), we did not observe the α5-α5, α5-β1, and α5-γ1 interactions reported by others (13). Rather, we observed a weak β1-γ1 interaction that was substantially strengthened by the addition of the α5 fragment, in line with the three-arm interaction model (15). In an effort to resolve the conflicting binding data obtained by SPR, we have now used size exclusion chromatography (SEC) to examine systematically the interactions between laminin short

* This work was supported by Wellcome Trust Senior Research Fellowship in Basic Biomedical Science 083942/Z/07/Z (to E. H.).
⌘ *Author's Choice*—Final version full access.
[1] To whom correspondence should be addressed: Dept. of Life Sciences, 4th Floor, Sir Ernst Chain Bldg., Imperial College London, London SW7 2AZ, UK. Tel.: 44-20-7594-7701; E-mail: e.hohenester@imperial.ac.uk.

[2] The abbreviations used are: LN, laminin N-terminal; LE, laminin-type epidermal growth factor-like; SPR, surface plasmon resonance; SEC, size exclusion chromatography; MALS, multiangle light scattering.

arm fragments. We found that authentic ternary network nodes can be reconstituted in solution, which makes them amenable to detailed structural studies.

EXPERIMENTAL PROCEDURES

Expression Vectors—All expression vectors were based on a modified pCEP-Pu vector (16), which adds an APLA sequence to the N terminus and an AAAHHHHHH sequence to the C terminus of the encoded proteins (after cleavage of the vector-encoded BM-40 secretion signal). The vectors coding for the LN-LEa1–4 regions of mouse laminin α1, α2, α5, β1, and γ1 chains have been described previously (15). The vectors encoding point mutants and chimeric proteins were made with strand overlap extension PCR and verified by DNA sequencing. The β1/γ1 chimera consists of β1 residues 22–332 (QEPEF . . . NSNAC) fused to γ1 residues 338–492 (LPCDC . . . KGCTP). The γ1/β1 chimera consists of γ1 residues 34–337 (AMDEC . . . SASEC) fused to β1 residues 333–509 (KKCNC . . . DGCRP).

Protein Production—Human embryonic kidney HEK293 c18 cells (American Type Culture Collection) were used for protein production. The cells were grown at 37 °C with 5% CO_2 in Dulbecco's modified Eagle's medium/nutrient mixture F-12 (Invitrogen) containing 10% fetal bovine serum, 2 mM glutamine, 10 units/ml penicillin, 100 μg/ml streptomycin, and 250 μg/ml Geneticin. The cells were transfected with the expression vectors using FuGENE 6 (Roche Diagnostics) and selected with 1 μg/ml puromycin (Sigma). Transfected cells were grown to confluence in HYPERFlask vessels (Corning) or 175-cm^2 EasyFlasks (Nunc), washed twice with PBS, and incubated with serum-free medium for up to 5 weeks with weekly medium exchanges. The serum-free conditioned media containing the recombinant laminin short arm fragments were adjusted to a final concentration of 20 mM HEPES (pH 7.5), 150 mM NaCl, 20 mM imidazole, and 2 mM $CaCl_2$. The proteins were purified from the adjusted medium by nickel affinity chromatography at 4 °C using 5-ml HisTrap FF columns (GE Healthcare) and an ÄKTA FPLC system (GE Healthcare), followed by SEC at 4 °C using a Superdex 200 16/60 column (GE Healthcare) and a running buffer consisting of 20 mM HEPES (pH 7.5), 150 mM NaCl, and 2 mM $CaCl_2$ (SEC buffer). The final protein yields were 5–10 mg/liter of medium for proteins produced in HYPERFlask vessels and 2–6 mg/liter for proteins produced in EasyFlasks. The purified proteins were concentrated to 3–4 mg/ml using Vivaspin concentrators (Sartorius), analyzed by SDS-PAGE and staining with Coomassie Blue (Generon), and snap-frozen for storage at −80 °C. Freshly thawed aliquots were used in all experiments. Protein concentrations were determined by spectrophotometry at 280 nm using extinction coefficients calculated from the primary sequence.

Analytical Size Exclusion Chromatography—The purified laminin short arm fragments were incubated either separately or in combination at a concentration of 18 μM (each fragment) for 1 h at room temperature. 200 μl of the incubated sample were loaded onto a Superdex 200 10/30 column (GE Healthcare) using an ÄKTA FPLC system and run at room temperature with SEC buffer at a flow rate of 0.25 ml/min. Different conditions were used in some experiments: incubation at 4 and 37 °C, chromatography at 4 °C, and 2 mM EDTA instead of 2 mM $CaCl_2$ in the incubation and running buffers. Molecular masses were determined by SEC combined with multiangle light scattering (SEC-MALS) using a Wyatt miniDAWN and Optilab T-rEX detector connected to a 1260 Infinity HPLC system (Agilent Technologies). Selected individual proteins (36 μM) and mixtures (18 μM each component) were incubated for 1 h at room temperature, and 100 μl were loaded onto the same Superdex 200 column used in all other experiments and run at room temperature with SEC buffer at a flow rate of 0.25 ml/min. The data were analyzed with ASTRA V software (Wyatt Technology Corp.) using dn/dc values of 0.185 and 0.145 ml/g for the polypeptide and polysaccharide fractions of the glycoproteins. Each consensus site for *N*-linked glycosylation was assumed to add 2 kDa of molecular mass. The mass of the polypeptide fraction of the glycoproteins was determined by the three-detector method (17) using extinction coefficients calculated from the primary sequence.

Surface Plasmon Resonance—The SPR experiment was carried out at 25 °C using a Biacore 3000 instrument (GE Healthcare). The β1 LN-LEa1–4 fragment was coupled to a CM5 chip in 10 mM sodium acetate (pH 4.5) according to the manufacturer's instructions. The reference cell was treated identically except that no protein was included. The running buffer was 20 mM NaHEPES (pH 7.5), 150 mM NaCl, and 2 mM $CaCl_2$ at a flow rate of 30 μl/min. The γ1 LN-LEa1–4 fragment was injected at concentrations ranging from 0.25 to 16 μM for 4 min, followed by a dissociation phase of 10 min, after which the resonance signal returned to its pre-injection level. The equilibrium binding constant was calculated from the sensorgrams using the Biacore software.

RESULTS

Purification of Laminin Short Arm Fragments—We recently described the production of recombinant short arm fragments of the laminin α1, α2, α5, β1, and γ1 chains, which contain the distal LN domain and the first four LE domains (LN-LEa1–4 fragments) (15). For the present biochemical study, we produced large quantities of these fragments and purified them to homogeneity. A stringent preparative SEC step was essential to obtain pure proteins, as most preparations contained a fraction of disulfide-linked oligomers that presumably arose from misfolded proteins with unpaired cysteines (data not shown). All purified short arm fragments gave single bands on reducing and nonreducing SDS-PAGE, with the exception of the α1 fragment (Fig. 1, *B* and *C*). The two bands of the α1 fragment correspond to different glycoforms because removal of the *N*-linked glycan with peptide *N*-glycosidase F produced a single sharp band at ~55 kDa (data not shown). Because the post-translational modifications produced by HEK293 cells closely resemble those of native mammalian glycoproteins, the fragments used in this study were expected to interact in a physiologically relevant manner.

Laminin Short Arm Interactions in Solution—We previously used SPR to demonstrate formation of a ternary laminin α5-β1-γ1 complex (15). However, we found that, after assembly of ternary complexes, the SPR sensor chips could not be regenerated without loss of activity of the immobilized laminin short arm fragments. This problem makes the use of SPR

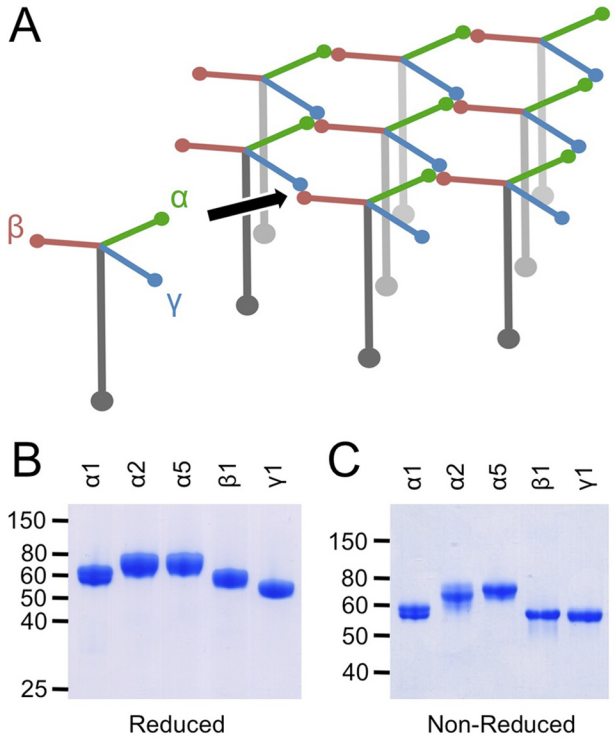

FIGURE 1. **Laminin short arms.** *A*, schematic drawing of the three-arm interaction model of laminin (10). The network nodes are formed by the short arm tips of one α, one β, and one γ chain. The long arm, which is a coiled coil of all three chains, mediates cell attachment. *B*, reducing SDS-PAGE of recombinant laminin short arm fragments. All fragments contain the globular LN domain followed by four LE domains (LN-LEa1–4) and a C-terminal His tag. The positions of selected molecular mass markers (in kDa) are indicated on the left. *C*, nonreducing SDS-PAGE of recombinant laminin short arm fragments. The positions of selected molecular mass markers (in kDa) are indicated on the left.

impractical for a detailed analysis of laminin network interactions. In the present study, we used analytical SEC to examine the interactions between the different laminin short arm fragments in solution. Although less well suited than SPR for detecting weak interactions, SEC is the method of choice for studying stable multicomponent complexes, especially when combined with MALS to determine their molecular masses (17).

When injected individually at 18 μM (~1 mg/ml) onto a SEC column, all laminin short arm fragments eluted in single peaks with elution volumes ranging from 13.6 to 14.6 ml (Fig. 2*A* and Table 1). Because of the elongated shape of the fragments, we did not correlate these elution volumes with those of globular molecular mass standards. Instead, we determined the molecular masses of the eluted α2, β1, and γ1 species by SEC-MALS and found them to be in good agreement with the calculated masses of the respective monomeric fragments (Fig. 3 and Table 2). Thus, the α2, β1, and γ1 short arm fragments do not stably self-interact in solution, and given their elution volumes, the same is very likely true of the α1 and α5 fragments.

We next analyzed all possible pairwise interactions between laminin short arm fragments. Equimolar mixtures (18 μM each component) were incubated for 1 h at room temperature and chromatographed at room temperature. For all but one combination, the elution profiles of the mixtures corresponded to the sum of the individual profiles, indicating that no stable com-

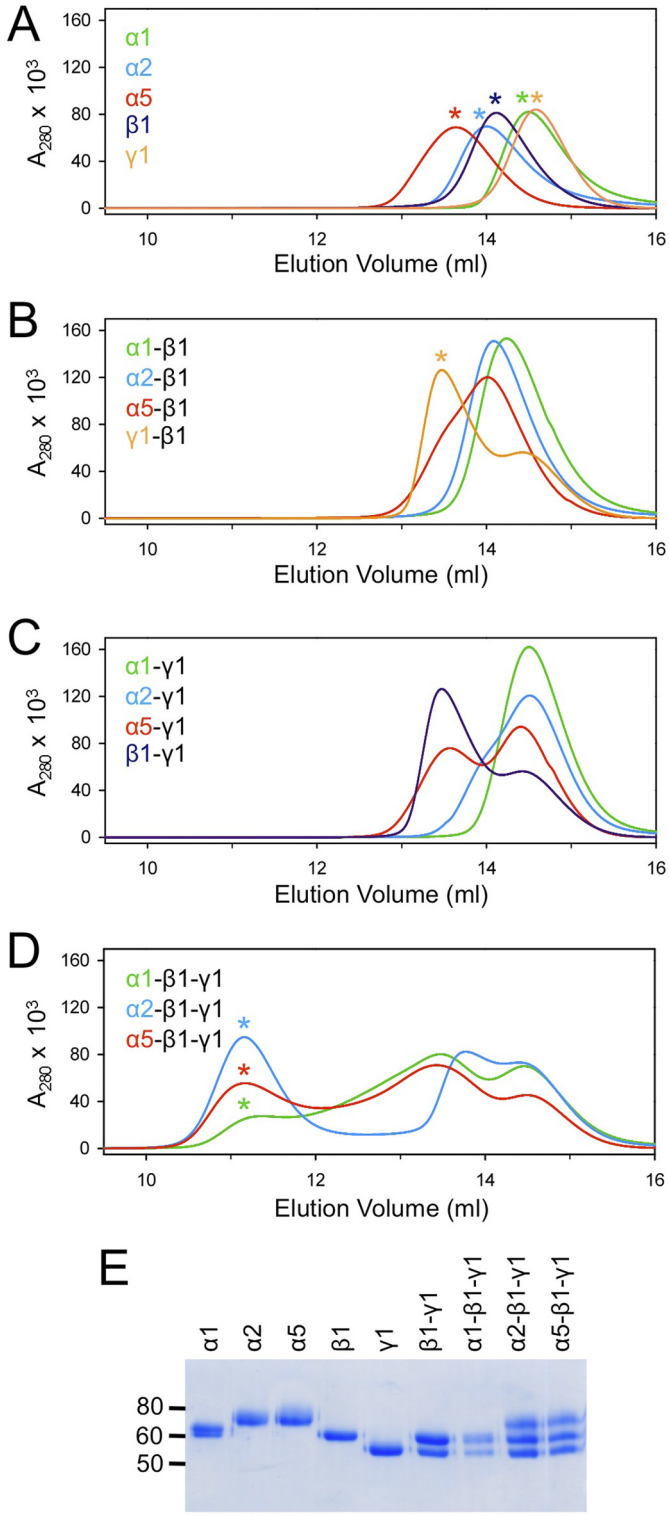

FIGURE 2. **SEC analysis of laminin short arm interactions.** Individual LN-LEa1–4 fragments (18 μM) or the indicated preincubated mixtures (18 μM each fragment) were injected onto a Superdex 200 column and run at room temperature with SEC buffer. *A*, individual fragments. *B*, binary mixtures with the β1 fragment. The peak eluting at ~13.5 ml contains the β1-γ1 complex. *C*, binary mixtures with the γ1 fragment. *D*, ternary mixtures. The peaks eluting at ~11 ml contain ternary complexes. *E*, reducing SDS-PAGE of peak fractions marked by *asterisks* in *A*, *B*, and *D*. The positions of selected molecular mass markers (in kDa) are indicated on the left.

plexes were formed (Fig. 2, *B* and *C*, and Table 1). Depending on the peak elution volumes of the respective isolated fragments, the non-interacting mixtures eluted either as two discrete peaks at the positions of the individual fragments (*e.g.* α5-γ1) or in a single (sometimes asymmetric) peak at an intermediate position. The single exception was the β1-γ1 complex mixture, which eluted earlier (13.5 ml) than either the β1 or γ1 fragment alone (14.1 and 14.6 ml, respectively). SDS-PAGE analysis of the major peak fraction at 13.5 ml confirmed the presence of both fragments, demonstrating a binary interaction of the laminin β1 and γ1 short arm fragments (Fig. 2*E*). The molecular mass of the β1-γ1 complex determined by SEC-MALS is lower than the mass calculated for a 1:1 complex (Fig. 3 and Table 2), suggesting that the peak at 13.5 ml contains a mixture of the complex and its free components. Such a situation would be expected for a weak β1-γ1 interaction with fast association and dissociation rates, as qualitatively observed in our previous SPR experiments (15). Using SPR, we determined a dissociation constant (K_d) of 22.3 ± 1.7 μM for the β1-γ1 complex (Fig. 4).

TABLE 1

Peak elution volumes of individual laminin short arm fragments and binary mixtures

An asymmetric peak with a shoulder at the front (sho) was observed for three mixtures.

	Fragment				
	α1	**α2**	**α5**	**β1**	**γ1**
	ml				
–	14.5	14.0	13.6	14.1	14.6
α1	–	14.2	13.5 + 14.2	14.3	14.5
α2		–	sho + 13.8	14.1	sho + 14.5
α5			–	sho + 14.0	13.6 + 14.5
β1				–	13.5 + 14.4
γ1					–

We then analyzed the three ternary mixtures: α1-β1-γ1, α2-β1-γ1, and α5-β1-γ1. Equimolar mixtures (18 μM each component) were incubated for 1 h at room temperature and chromatographed at room temperature. For all three mixtures, a new peak eluting at 11.2 ml was observed, in addition to peaks corresponding to the individual fragments and the previously characterized β1-γ1 complex (Fig. 2*D*). SDS-PAGE analysis of the 11.2-ml fraction confirmed the presence of all three short arm fragments in apparently equal quantities, demonstrating formation of ternary α-β-γ complexes (Fig. 2*E*, note that the α1 and β1 bands overlap). The molecular mass of the ternary α2-β1-γ1 complex was determined by SEC-MALS and is in excellent agreement with the calculated mass of a ternary complex of 1:1:1 stoichiometry (Fig. 3 and Table 2).

The amount of ternary complex eluting from the SEC column varied between the three laminin α chains (Fig. 2*D*). The α2-β1-γ1 complex mixture gave a discrete ternary complex peak that was separated from all other eluting species. The α5-β1-γ1 and α1-β1-γ1 complex mixtures gave a high detector signal across the entire 11–13-ml range, suggesting that these ternary complexes were dissociating more readily during the SEC runs. We do not expect the three ternary complexes to be fundamentally different, however, and the α2-β1-γ1 complex was selected for all subsequent experiments because of its highest (kinetic) stability.

The polymerization of full-length laminins in solution requires calcium and does not occur at 4 °C (6, 8, 10, 12). To determine whether these properties are shared by the α2, β1, and γ1 short arm fragments, we carried out SEC experiments without calcium and at different temperatures. When the α2-β1-γ1 complex mixture was incubated and chromato-

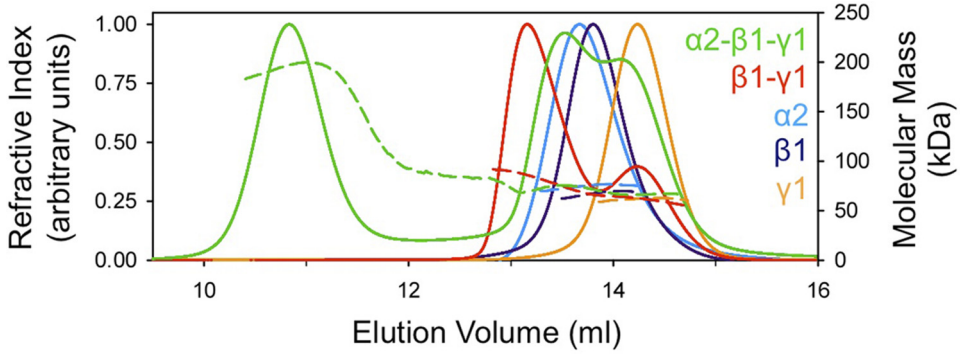

FIGURE 3. **SEC-MALS analysis of laminin short arm interactions.** Individual LN-LEa1–4 fragments (36 μM) or the indicated preincubated mixtures (18 μM each fragment) were injected onto a Superdex 200 column and run at room temperature with SEC buffer. The maximum in the refractive index detector signal (*solid lines*, *left y axis*) was set to 1.00 for each run. The experimental molecular masses (*dashed lines*, *right y axis*) refer to the glycoproteins (*i.e.* the sum of the polypeptide and oligosaccharide fractions).

TABLE 2

Calculated and experimentally determined molecular masses of selected laminin short arm fragments and mixtures

Protein	Molecular mass calculated from primary sequence	No. of consensus sites for *N*-linked glycosylation	Molecular mass of glycoprotein in SEC-MALS[a]	Molecular mass of polypeptide fraction in SEC-MALS[b]
	kDa		*kDa*	*kDa*
α2	55.5	6	79	56
β1	56.2	2	68	59
γ1	52.3	2	62	59
β1 + γ1	108.5	4	77[c]	67[c]
α2 + β1 + γ1	164.0	10	201	169

[a] Derived from the refractive index and light scattering signals.
[b] Derived from the A_{280}, refractive index, and light scattering signals (17). The concentration of the polypeptide fraction was determined using extinction coefficients calculated from the primary sequence.
[c] Mixture of the β1-γ1 complex and the free components (see "Results").

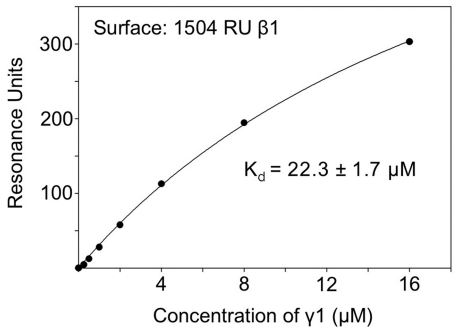

FIGURE 4. **SPR (Biacore) analysis of the laminin $\beta1$-$\gamma1$ interaction.** The $\beta1$ LN-LEa1–4 fragment was immobilized on a CM5 sensor chip, and the $\gamma1$ LN-LEa1–4 fragment was injected in SEC buffer. The resonance signals after equilibration (≥2 min after injection) were fitted by a binding isotherm with a dissociation constant of 22.3 ± 1.7 μM. *RU*, resonance units.

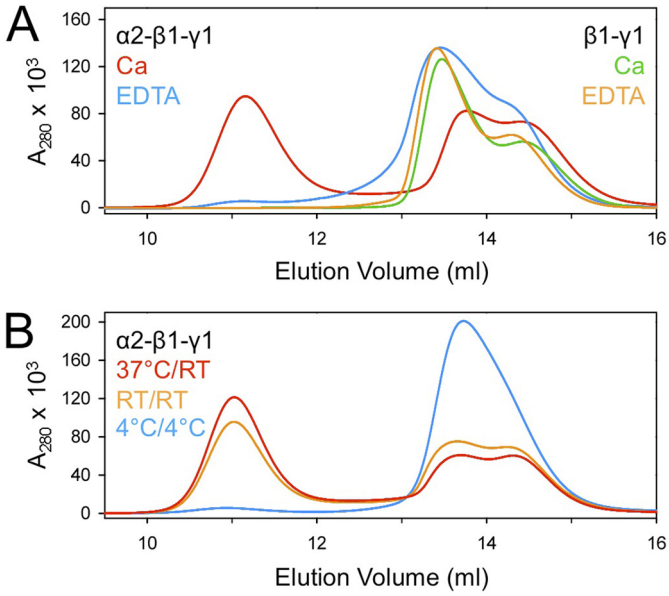

FIGURE 5. **Calcium and temperature dependence of laminin short arm interactions.** *A*, the indicated preincubated mixtures (18 μM each LN-LEa1–4 fragment) were injected onto a Superdex 200 column and run at room temperature (*RT*). The running buffer contained 20 mM HEPES (pH 7.5), 150 mM NaCl, and either 2 mM $CaCl_2$ or 2 mM EDTA. *B*, the $\alpha2$-$\beta1$-$\gamma1$ complex mixture (18 μM each fragment) was preincubated at the first indicated temperature and run at the second indicated temperature in the presence of calcium. The peaks eluting at ~11 and ~13.5 ml contain the ternary $\alpha2$-$\beta1$-$\gamma1$ and binary $\beta1$-$\gamma1$ complexes, respectively.

graphed in 2 mM EDTA, no ternary complex was observed (Fig. 5*A*). Interestingly, the binary $\beta1$-$\gamma1$ complex appeared to be unaffected by the removal of calcium ions. This result was confirmed by the near-identical elution profiles of the $\beta1$-$\gamma1$ complex mixture in 2 mM calcium and 2 mM EDTA (Fig. 5*A*). To study the temperature dependence of ternary complex formation, the $\alpha2$-$\beta1$-$\gamma1$ complex mixture was incubated and chromatographed at different temperatures. (For technical reasons, the SEC analysis was limited to 4 °C and room temperature.) Compared with incubation at room temperature, incubation at 37 °C slightly increased the amount of ternary complex formed. In sharp contrast, no ternary complex was formed at 4 °C (Fig. 5*B*). The combined results demonstrate that the ternary $\alpha2$-$\beta1$-$\gamma1$ short arm complex observed in SEC recapitulates the calcium and temperature dependence of laminin polymerization in solution and therefore represents an authentic node in the laminin network.

Structural Requirements for Laminin Short Arm Interactions—Having found that ternary nodes of the laminin network can be reconstituted in solution and analyzed by SEC, we sought to determine pertinent structural features of the stable $\alpha2$-$\beta1$-$\gamma1$ complex. An open question is whether the ternary network nodes are held together solely by interactions between the LN domains (as depicted in Fig. 1*A*) or by interactions between the LN domains of one chain and the LEa domains of another chain. Because the laminin LN domains cannot be produced without the adjacent LEa domains (13, 18), we decided to address this question by analyzing chimeric constructs of the $\beta1$ and $\gamma1$ chains. (We concentrated on these chains because of their unique binary interaction.) If only the LN domains were involved in network formation, a ternary complex with $\alpha2$ would be observed regardless of whether the $\beta1$ and $\gamma1$ LN domains are connected to their native LEa stalks or to the stalks of the respective other chain. If, on the other hand, the $\beta1$ or $\gamma1$ LEa stalks were involved as well, then no ternary complex would be formed with the chimeric constructs. We first made $\beta1/\gamma1$ and $\gamma1/\beta1$ chimeras in which only the LN domains were swapped. However, these proteins were poorly secreted by the HEK293 cells and prone to aggregation, probably because of structural perturbations in the artificial LN-LEa1 interfaces (data not shown). We next made a $\beta1/\gamma1$ chimera consisting of LN-LEa1 of $\beta1$ fused to LEa2–4 of $\gamma1$ and a $\gamma1/\beta1$ chimera consisting of LN-LEa1 of $\gamma1$ fused to LEa2–4 of $\beta1$. These proteins could be obtained in high purity (Fig. 6*B*) and eluted from the SEC column in single symmetrical peaks at a position corresponding to monomers (Fig. 7*A*). When analyzed by SEC, the $\beta1/\gamma1$ and $\gamma1/\beta1$ chimeras formed binary complexes with $\gamma1$ and $\beta1$, respectively, as well as with each other, whereas combinations with identical LN domains ($\beta1$-$\beta1/\gamma1$ and $\gamma1$-$\gamma1/\beta1$) did not interact (Fig. 7*B*). Most compellingly, the chimeras formed ternary complexes with the $\alpha2$ fragment in exactly the same way as the native short arm fragments (Fig. 7*C*). These results demonstrate that the LEa2–4 regions of the $\beta1$ and $\gamma1$ chains are dispensable for ternary complex formation and hence for laminin polymerization.

The experiments with the $\beta1/\gamma1$ and $\gamma1/\beta1$ chimeras did not rule out a possible involvement of the LEa1 domains in ternary complex formation. If the LEa1 domains were involved, a likely interaction site would be the LEa1 surface that is adjacent to the conserved face of the LN domain (14). We tested this hypothesis by introducing a bulky glycan at this location in the $\beta1$ short arm fragment (Fig. 6*A*). This was achieved by mutating LEa1 Arg-327 to asparagine, which creates a consensus site for *N*-linked glycosylation (R327N mutant). We also introduced a glycan at a location that we do not believe to be involved in ternary complex formation (H86N mutant) (Fig. 6*A*). Finally, to test the involvement of the conserved face of the $\beta1$ LN domain, we mutated Ser-68 to arginine (S68R mutant). Ser-68 is located near the tip of the $\beta1$ short arm and contributes to the large surface area of strictly conserved residues in the $\beta1$ LN domain (Fig. 6*A*). In the human $\beta2$ chain, the homologous S80R mutation causes Pierson syndrome (19, 20), and the $\beta1$ LN-LEa1–4

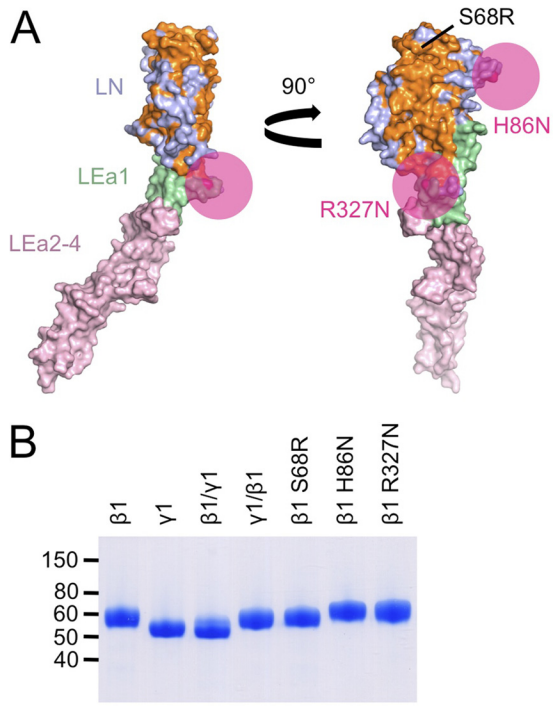

FIGURE 6. **Laminin short arm mutants.** *A*, location of point mutations in the laminin β1 short arm fragment. Shown are two orthogonal views of a surface representation of the β1 LN-LEa1–4 crystal structure (14). The LN domain is in *blue*, the LEa1 domain is in *green*, and the LEa2–4 domains are in *pink*. Strictly conserved residues in the LN domain are shown in *orange*. The location of the S68R mutation is indicated. *Semitransparent magenta circles* indicate the engineered glycans introduced by the H86N and R327N mutations. *B*, reducing SDS-PAGE of chimeric laminin short arm fragments and β1 mutants S68R, H86N, and R327N. The β1/γ1 chimera consists of LN-LEa1 of β1 fused to LEa2–4 of γ1; the γ1/β1 chimera consists of LN-LEa1 of γ1 fused to LEa2–4 of β1. The positions of selected molecular mass markers (in kDa) are indicated on the left.

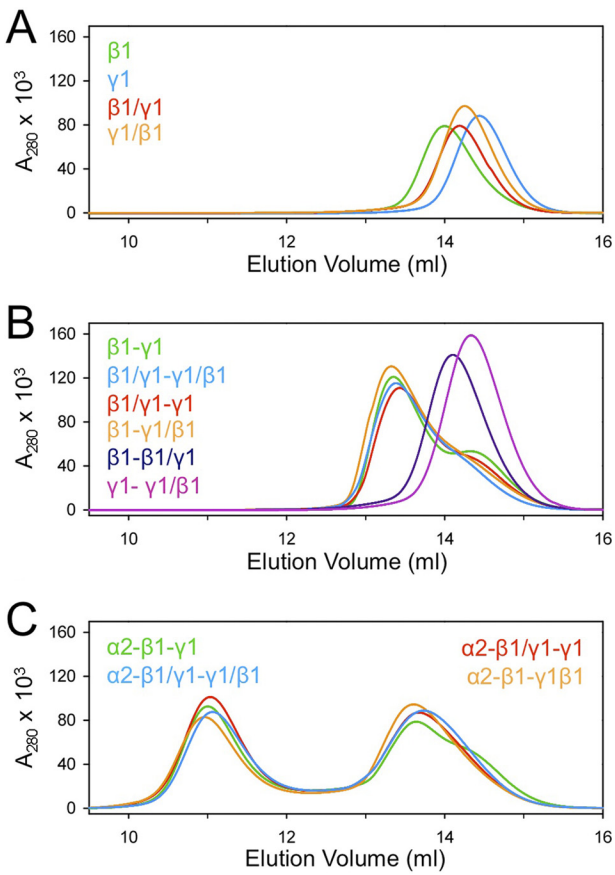

FIGURE 7. **SEC analysis of interactions involving chimeric laminin short arm fragments.** The β1/γ1 chimera consists of LN-LEa1 of β1 fused to LEa2–4 of γ1; the γ1/β1 chimera consists of LN-LEa1 of γ1 fused to LEa2–4 of β1. Individual fragments (18 μM) or the indicated preincubated mixtures (18 μM each fragment) were injected onto a Superdex 200 column and run at room temperature with SEC buffer. *A*, individual fragments. *B*, binary mixtures. The peaks eluting at ~13.5 ml contain binary complexes. *C*, ternary mixtures. The peaks eluting at ~11 ml contain ternary complexes.

crystal structure suggested that the mutation should be tolerated structurally (14).

The S68R, H86N, and R327N mutants of the β1 LN-LEa1–4 fragment were secreted by the HEK293 cells as well as the wild-type protein, indicating that the mutations did not perturb protein folding. SDS-PAGE of the purified proteins showed a mass increase for the H86N and R327N mutants, consistent with the addition of an *N*-linked glycan (Fig. 6*B*). Removal of the *N*-linked glycan with peptide *N*-glycosidase F produced a single sharp band at ~55 kDa for all β1 proteins (data not shown). When analyzed by SEC, the S68R mutant eluted identically to the wild-type protein, whereas the H86N and R327N mutants eluted ~0.3 ml earlier, again consistent with the addition of an *N*-linked glycan (Fig. 8*A*). All three β1 mutants formed binary complexes with γ1 (Fig. 8*B*). The β1 H86N and R327N mutants also formed ternary complexes with α2 and γ1, suggesting that the β1 LEa1 domain is unlikely to be involved in laminin network formation. In sharp contrast, the β1 S68R mutant failed to form a ternary complex with α2 and γ1 (Fig. 8*C*). This result demonstrates that the distal region of the β1 LN domain is essential for ternary complex formation, most likely by binding to the LN domain of the α chain.

DISCUSSION

The cross-shaped laminins polymerize in solution by a nucleation-propagation mechanism, similar to actin and tubulin (12, 21). According to the three-arm interaction model, the nodes in the laminin network are formed by the short arm tips of one α, one β, and one γ chain (10). Although this model is supported by a wealth of experimental data, the presumed ternary α-β-γ nodes have never been characterized biochemically. We now report that ternary complexes can be reconstituted from recombinant short arm fragments and exhibit all of the expected properties of laminin network nodes: (i) ternary complex formation is highly cooperative, with the only detectable intermediate being a weakly associated β-γ pair; (ii) ternary complexes have 1:1:1 stoichiometry; and (iii) ternary complexes do not form in the absence of calcium or at low temperature. These results provide compelling support for the three-arm interaction model and pave the way for detailed structural studies of the nodes in the laminin network.

Our previous, limited analysis of laminin short arm interactions by SPR revealed a weak interaction between the β1 and γ1 chains (with a K_d now determined to be 22.3 ± 1.7 μM) (Fig. 4) and a substantially more stable ternary α5-β1-γ1 complex with an apparent K_d of ~1 μM (15). These results fully agree with our new SEC data, which show a β1-γ1 complex rapidly equilibrating with its free components and a stable α5-β1-γ1 complex with a lifetime of many minutes (Figs. 2 and 3). We found no

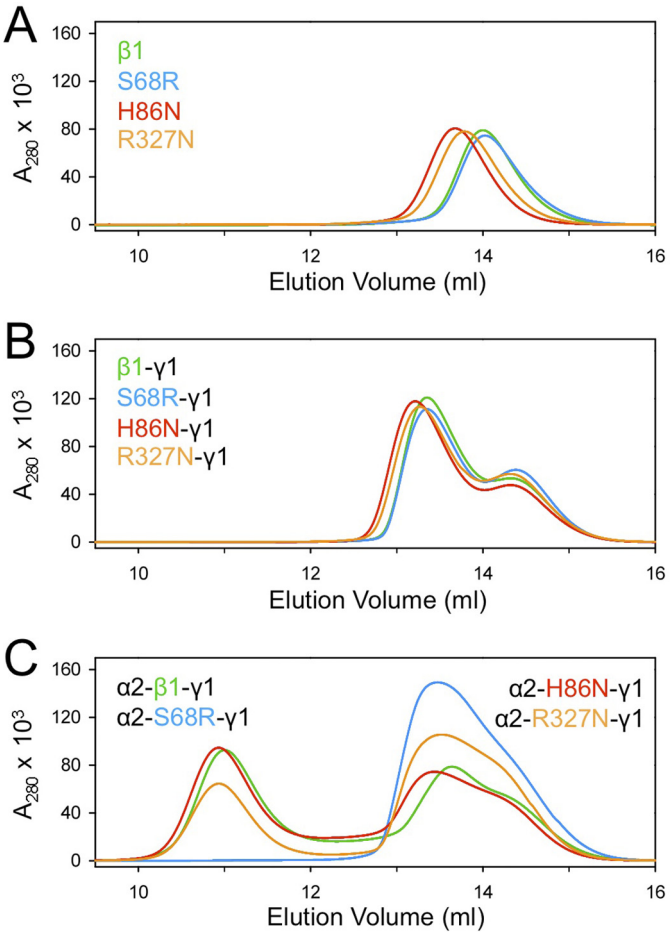

FIGURE 8. **SEC analysis of interactions involving wild-type and mutant laminin β1 short arm fragments.** Individual LN-LEa1–4 fragments (18 μM) or the indicated preincubated mixtures (18 μM each fragment) were injected onto a Superdex 200 column and run at room temperature with SEC buffer. *A*, individual fragments. *B*, binary mixtures with the γ1 fragment. The peaks eluting at ~13.5 ml contain binary complexes. *C*, ternary mixtures with the α2 and γ1 fragments. The peaks eluting at ~11 ml contain ternary complexes.

evidence of the strong α-α, α-β, and α-γ interactions reported by others (13). If these interactions had K_d values of 0.01–1 μM as claimed, they would not have escaped detection by SEC. The reasons for the conflicting results are unclear, but we are confident that our short arm fragments are properly folded and functional, given that they can be crystallized and inhibit laminin polymerization (14, 15).

The critical concentration of polymerization is lower for laminin-111 than for laminin-211, indicating that nucleation occurs more readily for the former (6, 11). We were initially surprised that the α1-β1-γ1 complex was less stable than the α2-β1-γ1 complex in our SEC experiments. Upon reflection, however, we concluded that there need not be a straightforward relationship between the critical concentration of polymerization and the stability of isolated network nodes in SEC. Most importantly, the nucleating species in laminin polymerization has not been characterized and may well be larger than three laminin molecules held together by a single node. Furthermore, we do not know whether the different elution profiles of the α1-β1-γ1 and α2-β1-γ1 complexes reflect differences in thermodynamic stability, kinetics, or both. A theoretical treatment of protein interactions in SEC suggests that the different elution profiles could be due to the α1-β1-γ1 complex forming and dissociating more rapidly than the α2-β1-γ1 complex (by a factor as small as 5-fold), without any difference in the equilibrium constants (22). The α1-β1-γ1 and α2-β1-γ1 complexes may also behave differently when studied at the higher temperature of the polymerization experiments. Finally, although it is clear that the LN domains are essential for polymerization, it cannot be excluded that laminin regions outside of the short arm tips somehow contribute to the stability of the laminin polymer.

Besides facilitating the purification of complexes for structural studies, SEC also provides a robust analytical tool to probe the structural requirements of ternary node formation. Previous analyses of sequence conservation suggested that the LE domains might not be involved in laminin network interactions (14, 15). Using SEC, we have shown here that neither the binary β1-γ1 interaction nor the ternary α2-β1-γ1 interaction requires the LEa2–4 domains of the β1 and γ1 chains. The β1 LEa1 domain does not appear to be involved either, given that a glycan engineered into the most likely interaction surface of LEa1 did not affect ternary complex formation (R327N mutant) (Fig. 8*C*). Although we cannot formally exclude that other LEa1 regions are involved, we think that only the LN domain of the β1 chain interacts with the α and γ chains in a ternary node. Consistent with this hypothesis, we found that mutation of a single surface residue in the β1 LN domain, Ser-68, abrogates ternary complex formation (Fig. 8*C*), and we previously showed that similar mutations in the α5 LN domain also destabilize the ternary complex (15). Thus, the collective evidence favors a model in which the nodes in the laminin network are formed exclusively by contacts between the LN domains. The role of the LE domains may be to ensure the appropriate spacing of nodes.

The S68R mutation in the β1 chain, which disrupted the ternary α2-β1-γ1 complex, corresponds to a homozygous S80R mutation in the closely related β2 chain that was identified in a patient with Pierson syndrome (20). In contrast to other Pierson syndrome mutations with no residual β2 expression, the S80R β2 chain was expressed quite normally in the kidney glomeruli (19). Indeed, judging from the normal secretion and SEC behavior of the β1 S68R mutant protein (Figs. 6*B* and 8*A*), the mutation does not perturb the LN domain structure. Thus, the β2 S80R mutation causes Pierson syndrome by an effect on laminin polymerization and not by the more common mechanism of reducing protein secretion or stability (20, 23).

In summary, reconstitution of laminin network nodes in solution has revealed how they are assembled. A weak and transient interaction of the β1 and γ1 chain LN domains is consolidated by the calcium-dependent addition of an α chain LN domain to form a ternary node of 1:1:1 stoichiometry. The reconstituted ternary nodes can be isolated for structure determination.

Acknowledgments—We thank Long Zhou for preliminary experiments and Jonathan Taylor for help with the SEC-MALS experiments.

REFERENCES

1. Yurchenco, P. D. (2011) Basement membranes: cell scaffoldings and signaling platforms. *Cold Spring Harb. Perspect. Biol.* **3,** a004911

2. Miner, J. H., and Yurchenco, P. D. (2004) Laminin functions in tissue morphogenesis. *Annu. Rev. Cell Dev. Biol.* **20,** 255–284
3. Aumailley, M., Bruckner-Tuderman, L., Carter, W. G., Deutzmann, R., Edgar, D., Ekblom, P., Engel, J., Engvall, E., Hohenester, E., Jones, J. C., Kleinman, H. K., Marinkovich, M. P., Martin, G. R., Mayer, U., Meneguzzi, G., Miner, J. H., Miyazaki, K., Patarroyo, M., Paulsson, M., Quaranta, V., Sanes, J. R., Sasaki, T., Sekiguchi, K., Sorokin, L. M., Talts, J. F., Tryggvason, K., Uitto, J., Virtanen, I., von der Mark, K., Wewer, U. M., Yamada, Y., and Yurchenco, P. D. (2005) A simplified laminin nomenclature. *Matrix Biol.* **24,** 326–332
4. Beck, K., Hunter, I., and Engel, J. (1990) Structure and function of laminin: anatomy of a multidomain glycoprotein. *FASEB J.* **4,** 148–160
5. Bruch, M., Landwehr, R., and Engel, J. (1989) Dissection of laminin by cathepsin G into its long-arm and short-arm structures and localization of regions involved in calcium-dependent stabilization and self-association. *Eur. J. Biochem.* **185,** 271–279
6. Cheng, Y. S., Champliaud, M. F., Burgeson, R. E., Marinkovich, M. P., and Yurchenco, P. D. (1997) Self-assembly of laminin isoforms. *J. Biol. Chem.* **272,** 31525–31532
7. McKee, K. K., Harrison, D., Capizzi, S., and Yurchenco, P. D. (2007) Role of laminin terminal globular domains in basement membrane assembly. *J. Biol. Chem.* **282,** 21437–21447
8. Paulsson, M. (1988) The role of Ca^{2+} binding in the self-aggregation of laminin-nidogen complexes. *J. Biol. Chem.* **263,** 5425–5430
9. Schittny, J. C., and Yurchenco, P. D. (1990) Terminal short arm domains of basement membrane laminin are critical for its self-assembly. *J. Cell Biol.* **110,** 825–832
10. Yurchenco, P. D., and Cheng, Y. S. (1993) Self-assembly and calcium-binding sites in laminin. A three-arm interaction model. *J. Biol. Chem.* **268,** 17286–17299
11. Yurchenco, P. D., Cheng, Y. S., and Colognato, H. (1992) Laminin forms an independent network in basement membranes. *J. Cell Biol.* **117,** 1119–1133
12. Yurchenco, P. D., Tsilibary, E. C., Charonis, A. S., and Furthmayr, H. (1985) Laminin polymerization *in vitro*. Evidence for a two-step assembly with domain specificity. *J. Biol. Chem.* **260,** 7636–7644
13. Odenthal, U., Haehn, S., Tunggal, P., Merkl, B., Schomburg, D., Frie, C., Paulsson, M., and Smyth, N. (2004) Molecular analysis of laminin N-terminal domains mediating self-interactions. *J. Biol. Chem.* **279,** 44504–44512
14. Carafoli, F., Hussain, S. A., and Hohenester, E. (2012) Crystal structures of the network-forming short-arm tips of the laminin β1 and γ1 chains. *PLoS ONE* **7,** e42473
15. Hussain, S. A., Carafoli, F., and Hohenester, E. (2011) Determinants of laminin polymerization revealed by the structure of the α5 chain amino-terminal region. *EMBO Rep.* **12,** 276–282
16. Kohfeldt, E., Maurer, P., Vannahme, C., and Timpl, R. (1997) Properties of the extracellular calcium binding module of the proteoglycan testican. *FEBS Lett.* **414,** 557–561
17. Wen, J., Arakawa, T., and Philo, J. S. (1996) Size-exclusion chromatography with on-line light-scattering, absorbance, and refractive index detectors for studying proteins and their interactions. *Anal. Biochem.* **240,** 155–166
18. Garbe, J. H., Göhring, W., Mann, K., Timpl, R., and Sasaki, T. (2002) Complete sequence, recombinant analysis and binding to laminins and sulphated ligands of the N-terminal domains of laminin α3B and α5 chains. *Biochem. J.* **362,** 213–221
19. Lehnhardt, A., Lama, A., Amann, K., Matejas, V., Zenker, M., and Kemper, M. J. (2012) Pierson syndrome in an adolescent girl with nephrotic range proteinuria but a normal GFR. *Pediatr. Nephrol.* **27,** 865–868
20. Matejas, V., Hinkes, B., Alkandari, F., Al-Gazali, L., Annexstad, E., Aytac, M. B., Barrow, M., Bláhová, K., Bockenhauer, D., Cheong, H. I., Maruniak-Chudek, I., Cochat, P., Dötsch, J., Gajjar, P., Hennekam, R. C., Janssen, F., Kagan, M., Kariminejad, A., Kemper, M. J., Koenig, J., Kogan, J., Kroes, H. Y., Kuwertz-Bröking, E., Lewanda, A. F., Medeira, A., Muscheites, J., Niaudet, P., Pierson, M., Saggar, A., Seaver, L., Suri, M., Tsygin, A., Wühl, E., Zurowska, A., Uebe, S., Hildebrandt, F., Antignac, C., and Zenker, M. (2010) Mutations in the human laminin β2 (*LAMB2*) gene and the associated phenotypic spectrum. *Hum. Mutat.* **31,** 992–1002
21. Oosawa, F., and Kasai, M. (1962) A theory of linear and helical aggregations of macromolecules. *J. Mol. Biol.* **4,** 10–21
22. Stevens, F. J. (1989) Analysis of protein-protein interaction by simulation of small-zone size exclusion chromatography. Stochastic formulation of kinetic rate contributions to observed high-performance liquid chromatography elution characteristics. *Biophys. J.* **55,** 1155–1167
23. Chen, Y. M., Kikkawa, Y., and Miner, J. H. (2011) A missense *LAMB2* mutation causes congenital nephrotic syndrome by impairing laminin secretion. *J. Am. Soc. Nephrol.* **22,** 849–858